International Journal of
Advanced Structural Engineering
a SpringerOpen Journal

ORIGINAL RESEARCH   **Open Access**

Vibration of wavy single-walled carbon nanotubes based on nonlocal Euler Bernoulli and Timoshenko models

Payam Soltani[1,2*], Amir Kassaei[1], Mohammad Mehdi Taherian[3] and Anooshiravan Farshidianfar[2]

Abstract

The transverse vibration of a single-walled carbon nanotube (SWCNT) with light waviness along its axis is modeled by the nonlocal Euler-Bernoulli and Timoshenko beam theory. Unlike the Euler-Bernoulli beam model (EBM), the effects of transverse shear deformation and rotary inertia are considered within the framework of the Timoshenko beam model (TBM). The surrounding elastic medium is described as both Winkler-type and Pasternak-type foundation models. The governing equations are derived using Hamilton's principle, and the Galerkin method is applied to solve these equations. According to this study, the results indicate that the frequency calculated by TBM is lower than that obtained by EBM. Detailed results show that the importance of transverse shear deformation and rotary inertia become more significant for stocky SWCNTs with clamped-clamped boundary conditions. Moreover, the influences of the amplitude of waviness, nonlocal parameter, medium constants, boundary conditions and aspect ratio are analyzed and discussed. It is shown that waviness in the curved SWCNT causes an obvious increase in the natural frequency in comparison with the straight SWCNT, especially for a compliant medium, pinned-pinned boundary condition, short SWCNT and large nonlocal coefficient.

Keywords: Curved single-walled carbon nanotubes, Vibration, Timoshenko beam model, Nonlocal elasticity theory

Introduction

The discovery of carbon nanotubes (CNTs) by Ijima (Iijima 1991) in the past decade has stimulated research communities in nanotechnology and the development of nano-scale functional devices designed for, and devoted to, carbon nanostructures. The superior mechanical, thermal and electrical properties of CNTs have been investigated in extensive research. For instant, the results show that in its mechanical properties, CNTs have exhibited excellent mechanical stiffness and strength (Dresselhaus et al. 2004; Treacy et al. 1996; Walgraef 2007). These properties have caused CNTs to become one of the most promising materials for nano-electronics, nano-devices and nano-composites (Chen et al. 2004; Hafner et al. 1999; Nishide et al. 2003; Tsukagoshi et al. 2002).

Recently, the mechanical behavior has become the main topic of interest. Therefore, several studies have been done to investigate the vibration of CNTs, since it is essential to understand their dynamical behavior. There are two main categories for simulating the mechanical and physical properties of CNTs: the first is atomic modeling, which includes such techniques as classical molecular dynamics (MD). This method is time consuming, complex, expensive in computational cost and limited to maximum system sizes of about 10^9 atoms (Lau et al. 2004; Liew et al. 2004). The second type is continuum-based modeling, which includes elastic beam models (Yoon et al. 2005; Zhang et al. 2006; Wang et al. 2008; Kuang et al. 2009) and elastic shell theories (Yakobson et al. 1997; Nguyen et al. 2009; Yan et al. 2009; Liew & Wang 2007). For the beam models, the Euler-Bernoulli beam model (EBM) (Fu et al. 2006; Chaterjee & Pohit 2009; Chowdhury et al. 2009) as well as the Timoshenko beam model (TBM) (Hsu et al. 2008; Wang et al. 2006; Lee & Chang 2009; Mahdavi et al. 2011) have been widely employed. The EBM ignores the

* Correspondence: payam.soltani@gmail.com
[1]Department of Mechanical Engineering, Semnan Branch, Islamic Azad University, Semnam, Iran
[2]Department of Mechanical Engineering, Ferdowsi University of Mashhad, Mashhad, Iran
Full list of author information is available at the end of the article
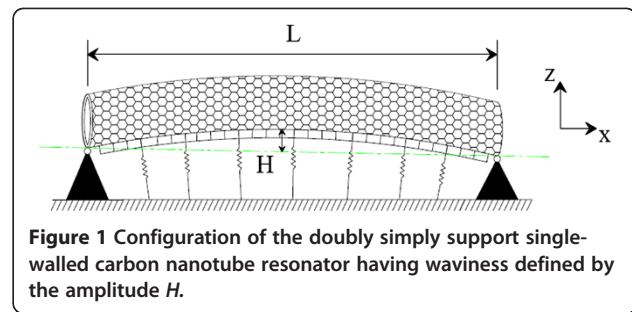
effect of rotary inertia and transverse shear deformation and is applicable to analysis of vibrational characteristics of CNTs. Therefore, the TBM model offers a more precise model compared with the Euler-Bernoulli theory (Rao 2007). The above mentioned literature cannot consider the nano-scale effect on the formulation. The small-scale effect in elasticity is described by assuming that the stress at a point is a function, not only of the strain at that point, but the stress at all reference points and is a function of strain field at every point in the body, as proposed in Eringen's nonlocal elasticity theory (Eringen 1983). Nowadays, many studies have been devoted to analysis of the vibration of CNTs, based on this non-classical theory (Murmu & Pradhan 2009a; Şimşek 2011; Mehdipour et al. 2011; Wang & Ni 2008; Yang et al. 2010; Murmu & Pradhan 2009b).

Most previous theoretical studies are for straight nanotubes, but theoretic and experimental investigations show that the CNTs are not straight in the environment. There are few investigations performed to examine the vibration of curved CNTs. For example, Joshi et al. (Joshi et al. 2010) investigated the vibrational response analysis of carbon nanotubes with their waviness treated as a thin shell. Furthermore, Mayoof and Hawwa (Hawwa & Mayoof 2009) used classical EBM to study the dynamics of the CNT when it acted as the first-mode resonator, with a focus on the chaotic behavior of a curved carbon nanotube under harmonic excitation.

In the present study, both nonlocal Euler-Bernoulli and Timoshenko beam theories are used to simulate the linear transverse vibration of an embedded SWCNT with waviness. To the best of our knowledge, no previous work has been done concerning the vibration behavior of curved CNTs based on TBM. The surrounding elastic medium is described as a Winkler and Pasternak model. The equations of motion are derived by Hamilton's principle, and they are solved using the Galerkin method to obtain fundamental frequencies. The importance of rotary inertia and transverse shear deformation has been explored by comparing the natural frequencies for both EBM and TBM theories. In addition, the effects of amplitude of curvature on the fundamental frequency are discussed. Moreover, the variation of frequency has been considered based on the different parameters such as the surrounding elastic medium, the boundary conditions, the aspect ratio of the SWCNT and the nonlocal coefficient.

Modeling

The system under consideration in Figure 1 is a doubly simply supported ends SWCNT with immovable ends, length L, initial waviness amplitude H, Young's modulus E, shear modulus G, cross-sectional area A, cross-sectional moment I, mass moment inertia J and mass per unit length m. The surrounding elastic medium is simulated by both

Figure 1 Configuration of the doubly simply support single-walled carbon nanotube resonator having waviness defined by the amplitude H.

Pasternak-type and Winkler-type variables. The Winkler-type elastic foundation is assumed to act as a vertical linear spring while the Pasternak-type explains the transverse shear stress due to interaction between SWCNT and shear deformation of its medium (Murmu & Pradhan 2009b). This medium is defined by K_W and K_G to represent the Winkler modulus and Pasternak shear modulus of the elastic medium, respectively.

Nonlocal Timoshenko Beam Theory

Because it considers the transverse shear deformation and rotary inertia, TBM provides more reliable results compared to other elastic beam theories. Thus, based on this theory, the displacement field in x-z plane and at any point in the body is as

$$\tilde{U}(x,z,t) = U(x,t) + z\psi(x,t), \tilde{W}(x,z,t) = W(x,t) \tag{1}$$

Where x is the longitude coordinate, z the coordinate measured from the mid-plane of the beam and t is time. Moreover, $U(x,t)$ and $W(x,t)$ are axial and transverse displacement components in the mid-plane, respectively, and ψ is the rotation of the cross-section.

According to Eq. (1), the linear and nonzero strains are expressed as

$$\varepsilon_{xx} = \frac{\partial U}{\partial x} + \frac{\partial R}{\partial x}\frac{\partial W}{\partial x} + z\left(\frac{\partial \psi}{\partial x}\right), \varepsilon_{zz} = 0, \varepsilon_{xz} = \frac{\partial W}{\partial x} + \psi \tag{2}$$

Where, ε_{xx} is the axial strain, ε_{xz} is the shear strain and $R(x)$ represents the small rise function that is described as $R(x) = H\sin(\pi x/L)$.

The potential energy of strain V_s is given by

$$V_s = \frac{1}{2}\int_0^L \int_A (\sigma_{xx}\varepsilon_{xx} + \sigma_{xz}\varepsilon_{xz})dAdx \tag{3}$$

Where, σ_{xx} and σ_{xz} are normal stress and shear stress, respectively. By substituting Eq. (2) into Eq. (3), the strain energy V_s can be written as

$$V_s = \frac{1}{2} \int_0^L \int_A \left\{ \sigma_{xx} \left[\frac{\partial U}{\partial x} + \frac{\partial \phi}{\partial x} \frac{\partial W}{\partial x} + z \left(\frac{\partial \psi}{\partial x} \right) \right] + \sigma_{xz} \left(\frac{\partial W}{\partial x} + \psi \right) \right\} dA dx$$
$$= \frac{1}{2} \int_0^L \left\{ N_x \left[\frac{\partial U}{\partial x} + \frac{\partial \phi}{\partial x} \frac{\partial W}{\partial x} \right] + M_x \left(\frac{\partial \psi}{\partial x} \right) + Q_x \left(\frac{\partial W}{\partial x} + \psi \right) \right\} dx$$

(4)

The axial resultant force N_x, bending moment M_x and transverse resultant force Q_x can be obtained from

$$N_x = \int_A \sigma_{xx} dA, M_x = \int_A \sigma_{xx} z dA, Q_x = \int_A \sigma_{xz} dA. \quad (5)$$

The kinetic energy T is calculated from

$$T = \frac{1}{2} m \int_0^L \left(\frac{\partial W}{\partial t} \right)^2 dx + \int_0^L J \frac{\partial \psi}{\partial t} dx. \quad (6)$$

The work V_e done by external load can be expressed as

$$V_e = \int_0^L f_e W dx. \quad (7)$$

f_e indicates the external load and corresponds to

$$f_e = -K_W W + K_G \frac{\partial^2 W}{\partial x^2}. \quad (8)$$

According to the nonlocal elasticity theory of Eringen, shear force and bending moment in the nonlocal beam theory are different from those in the classical TBM due to the nonlocal constitutive equations (Eringen 2002), The one-dimensional form for nonlocal constitutive relations can be approximated as

$$\sigma_{xx} - (e_0 a)^2 \frac{d^2 \sigma_{xx}}{dx^2} = E \varepsilon_{xx} \quad (9-a)$$

$$\sigma_{xz} - (e_0 a)^2 \frac{d^2 \sigma_{xz}}{dx^2} = G \varepsilon_{xz}. \quad (9-b)$$

It should be noted that by setting the nonlocal parameter $e_0 a = 0$ the constitutive relations in classical elasticity theories can be recovered.

Substituting Eqs. (4), (6) and (7) into Hamilton's principle $\int_0^L (\delta T - \delta V_s + \delta V_e) dt = 0$, integrating by parts and setting the coefficients of δW, δU and $\delta \psi$ to zero leads to the differential equations of motion as

$$\delta U : \frac{\partial N_x}{\partial x} = 0 \quad (10-a)$$

$$\delta W : \frac{\partial^2 M_x}{\partial x^2} = m \left(\frac{\partial^2 W}{\partial t^2} \right) - \frac{\partial}{\partial x} \left(N_x \frac{\partial W}{\partial x} \right) - \frac{\partial}{\partial x}$$
$$\left(N_x \frac{\partial Z}{\partial x} \right) - \frac{\partial Q_x}{\partial x} + f_e$$

(10 − b)

$$\delta \psi : \frac{\partial Q_x}{\partial x} = J \frac{\partial^2 \psi}{\partial t^2} - \frac{\partial M}{\partial x} + Q_x \quad (10-c)$$

and corresponding boundary conditions at beam ends $(x = 0, L)$ entail

$$U = 0 \, or \, N_x = 0, \; W = 0 \, or \, Q_x = 0, \; \psi = 0 \, or \, M_x = 0.$$

(11)

By using Eqs. (2), (5) and (9), the normal resultant force, bending moment and shear force can be expressed as

$$N_x - (e_0 a)^2 \frac{\partial^2 N_x}{\partial x^2} = EA \left(\frac{\partial U}{\partial x} + \frac{\partial R}{\partial x} \frac{\partial W}{\partial x} \right) \quad (12-a)$$

$$M_x - (e_0 a)^2 \frac{\partial^2 M_x}{\partial x^2} = EI \frac{\partial \psi}{\partial x} \quad (12-b)$$

$$Q_x - (e_0 a)^2 \frac{\partial^2 Q_x}{\partial x^2} = kAG \left(\frac{\partial W}{\partial x} + \psi \right). \quad (12-c)$$

Where k is the shear correction factor, depending on the shape of the cross-section of the beam. By sequence substituting Eq. (10-a), (10-b) and (10-c) into Eqs. (12-a), (12-b) and (12-c), the explicit expressions of nonlocal normal resultant force N_x, bending moment M_x and shear force Q_x can be obtained as

$$N_x = EA \left(\frac{\partial U}{\partial x} + \frac{\partial R}{\partial x} \frac{\partial W}{\partial x} \right) \quad (13-a)$$

$$M_x = EI \frac{\partial \psi}{\partial x} + (e_0 a)^2$$
$$\left(m \frac{\partial^2 W}{\partial t^2} - \frac{\partial}{\partial x} \left(N_x \frac{\partial R}{\partial x} \right) + J \frac{\partial^3 \psi}{\partial t^2 \partial x} - f_e \right)$$

(13 − b)

$$Q_x = kAG\left(\frac{\partial W}{\partial x} + \psi\right) + (e_0 a)^2$$
$$\left(m\frac{\partial^3 W}{\partial x \partial t^2} - \frac{\partial^2}{\partial x^2}\left(N_x\frac{\partial R}{\partial x}\right) - \frac{\partial f_e}{\partial x}\right).$$

$$(13-c)$$

The governing equation for nonlocal SWCNTs can be derived by inserting Eqs. (13) into Eqs. (10)

$$EA\left(\frac{\partial^2 U}{\partial x^2} + \frac{\partial^2 R}{\partial x^2}\frac{\partial W}{\partial x} + \frac{\partial R}{\partial x}\frac{\partial^2 W}{\partial x^2}\right) = 0 \qquad (14-a)$$

$$EA\left[(e_0 a)^2 \Sigma_1 - \Sigma_2\right] - (KAG + K_G)\frac{\partial^2 W}{\partial x^2}$$
$$+ m\frac{\partial^2 W}{\partial t^2} - kAG\frac{\partial \psi}{\partial x} + K_W W - m\frac{\partial^4 W}{\partial x^2 \partial t^2}$$
$$- K_W\frac{\partial^2 W}{\partial x^2} + K_G\frac{\partial^4 W}{\partial x^4} = 0 \qquad (14-b)$$

$$J\left[(e_0 a)^2\frac{\partial^4 \psi}{\partial x^2 \partial t^2} - \frac{\partial^2 \psi}{\partial t^2}\right] - KAG\left(\frac{\partial W}{\partial x} + \psi\right) + EI\frac{\partial^2 \psi}{\partial x^2} = 0$$

$$(14-c)$$

Where

$$\Sigma_1 = \frac{\partial R}{\partial x}\left(\frac{\partial^4 U}{\partial x^4} + 2\frac{\partial^4 R}{\partial x^4}\frac{\partial W}{\partial x} + 6\frac{\partial^3 R}{\partial x^3}\frac{\partial^2 W}{\partial x^2}\right.$$
$$\left. + 6\frac{\partial^2 R}{\partial x^2}\frac{\partial^3 W}{\partial x^3} + \frac{\partial R}{\partial x}\frac{\partial^4 W}{\partial x^4}\right)$$
$$+ \frac{\partial^2 R}{\partial x^2}\left(3\frac{\partial^3 U}{\partial x^3} + 6\frac{\partial^3 R}{\partial x^3}\frac{\partial W}{\partial x} + 6\frac{\partial^2 R}{\partial x^2}\frac{\partial^2 W}{\partial x^2}\right)$$
$$+ 3\frac{\partial^3 R}{\partial x^3}\frac{\partial^2 U}{\partial x^2} + \frac{\partial^4 R}{\partial x^4}\frac{\partial U}{\partial x} \qquad (15-a)$$

$$\Sigma_2 = \frac{\partial R}{\partial x}\left(\frac{\partial^2 U}{\partial x^2} + 2\frac{\partial^2 R}{\partial x^2}\frac{\partial W}{\partial x} + \frac{\partial R}{\partial x}\frac{\partial^2 W}{\partial x^2}\right) - \frac{\partial^2 R}{\partial x^2}\frac{\partial U}{\partial x}.$$

$$(15-b)$$

By integrating over the domain [0-L] from Eq. (14-a), displacement along x axes can be obtained as

$$U = -\int_0^x \left[\frac{1}{2}\left(\frac{\partial W}{\partial x}\right)^2 + \frac{\partial R}{\partial x}\frac{\partial W}{\partial x}\right]dx$$
$$+ x\frac{1}{L}\int_0^L\left[\frac{1}{2}\left(\frac{\partial W}{\partial x}\right)^2 + \frac{\partial R}{\partial x}\frac{\partial W}{\partial x}\right]dx. \qquad (16)$$

Eqs. (14-a), (14-b) and 14-c) are consistent basic equations of the curved TBM. By using Eq. (16) and eliminating ψ, Eqs. (14) are summarized as an uncoupled equation as

$$\frac{(e_0 a)^4}{kAG}\left(-\frac{EJA}{L}\frac{\partial^6 R}{\partial x^6}\int_0^L\frac{\partial R}{\partial x}\frac{\partial W}{\partial x}dx + JK_W\frac{\partial^6 W}{\partial x^4 \partial t^2}\right.$$
$$\left. - K_G\frac{\partial^8 W}{\partial x^6 \partial t^2} + Jm\frac{\partial^8 W}{\partial x^4 \partial t^4}\right)\frac{-b \pm \sqrt{b^2 - 4ac}}{2a}$$
$$+ \frac{(e_0 a)^2}{kAG}\left[-\frac{2JEA}{L}\frac{\partial^4 R}{\partial x^4}\int_0^L\frac{\partial R}{\partial x}\frac{\partial^3 W}{\partial x \partial t^2}dx\right.$$
$$+ \left(EI\frac{\partial^6 R}{\partial x^6} - kAG\frac{\partial^4 R}{\partial x^4}\right)\frac{EA}{L}\int_0^L\frac{\partial R}{\partial x}\frac{\partial W}{\partial x}dx$$
$$+ 2JK_W\frac{\partial^4 W}{\partial x^2 \partial t^2} + Jm\frac{\partial^6 W}{\partial x^2 \partial t^4} - mEI\frac{\partial^6 W}{\partial x^4 \partial t^2}$$
$$\left. - JK_G\frac{\partial^6 W}{\partial x^4 \partial t^2} + EI\left(K_G\frac{\partial^6 W}{\partial x^6} - K_W\frac{\partial^4 W}{\partial x^4}\right)\right]$$
$$+ (e_0 a)^2\left(J\frac{\partial^6 W}{\partial x^4 \partial t^2} + m\frac{\partial^4 W}{\partial x^2 \partial t^2} - K_G\frac{\partial^4 W}{\partial x^4} + K_W\frac{\partial^2 W}{\partial x^2}\right)$$
$$+ \frac{1}{KAG}\left[\left(-EI\frac{\partial^4 R}{\partial x^4} + kAG\frac{\partial^2 R}{\partial x^2}\right)\frac{EA}{L}\int_0^L\frac{\partial R}{\partial x}\frac{\partial W}{\partial x}dx\right.$$
$$+ \frac{JEA}{L}\frac{\partial^2 R}{\partial x^2}\int_0^L\frac{\partial R}{\partial x}\frac{\partial^3 W}{\partial x \partial t^2}dx + (JK_G + mEI)\frac{\partial^4 W}{\partial x^2 \partial t^2}$$
$$\left. - (EIK_G + Jm)\frac{\partial^4 W}{\partial x^4} + (EI - J)K_W\frac{\partial^4 W}{\partial x^4}\right]$$
$$+ J\frac{\partial^4 W}{\partial x^2 \partial t^2} + EI\frac{\partial^4 W}{\partial x^4} - m\frac{\partial^2 W}{\partial x^2} + K_G\frac{\partial^2 W}{\partial x^2}$$
$$+ K_W W = 0. \qquad (17)$$

Nonlocal Euler-Bernoulli Beam Model

The governing equation of EBM contains only the deflection of the beam because the effects of transverse shear deformation and rotary inertia are ignored. Therefore, the linear strain–displacement relations for curved Euler beam are expressed as

$$\varepsilon_{xx} = \frac{\partial U}{\partial x} + \frac{\partial R}{\partial x}\frac{\partial W}{\partial x} - z\left(\frac{\partial^2 W}{\partial x^2}\right), \varepsilon_{zz} = \varepsilon_{xz} = 0. \qquad (18)$$

By performing a similar approach to that presented for the TBM, the differential equation that governs the vibration of the curved SWCNT based on the EBM is obtained as

$$EI\frac{\partial^4 W}{\partial x^4} + m\left(\frac{\partial^2 W}{\partial t^2} - (e_0 a)^2 \frac{\partial^4 W}{\partial x^2 \partial t^2}\right)$$

$$+ K_G\left((e_0 a)^2 \frac{\partial^4 W}{\partial x^4} - \frac{\partial^2 W}{\partial x^2}\right)$$

$$+ K_W\left(W - (e_0 a)^2 \frac{\partial^2 W}{\partial x^2}\right)$$

$$= EA\left(\frac{\partial^2 R}{\partial x^2} - (e_0 a)^2 \frac{\partial^4 R}{\partial x^4}\right) \int_0^x \left(\frac{\partial R}{\partial x}\frac{\partial W}{\partial x}\right) dx. \tag{19}$$

The boundary conditions for SWCNTs with immovable ends can be considered as

$$W = \psi = 0 \quad x = 0, L. \tag{20}$$

For clamped ends and

$$W = 0,$$
$$M_x = EI\frac{\partial \psi}{\partial x} + (e_0 a)^2\left(m\frac{\partial^2 W}{\partial t^2} - \frac{\partial}{\partial x}\left(N_x\frac{\partial R}{\partial x}\right)\right.$$
$$\left. + J\frac{\partial^3 \psi}{\partial t^2 \partial x} + K_W W - K_G\frac{\partial^2 W}{\partial x^2}\right) = 0 \quad x = 0, L \tag{21}$$

For pinned ends.

Solution Method

In this study, the free vibration equation of the curved SWCNT has been investigated by using the nonlocal TBM and EBM. The influences of transverse shear deformation and rotary inertia on the vibration frequencies are investigated by comparing the TBM results with those based on the EBM.

For rewriting the governing equations in a non-dimensional form, introducing the following dimensionless quantities is important

$$\tau = t\omega, \omega = \sqrt{\frac{EI}{mL^4}}, \Omega = \frac{\omega}{\omega_0} \xi = \frac{x}{L},$$
$$w = \frac{W}{L}, b = \frac{J}{mL^2} r = \frac{R}{L}, s = \frac{AL^2}{I},$$
$$k_W = \frac{K_W L^4}{EI}, h = \frac{H}{L} k_G = \frac{K_G L^2}{EI}, e_n = \frac{e_0 a}{L}, \tag{22}$$
$$p = \sqrt{\frac{EI}{kAGL^2}}, k = \frac{2(1+v)}{4+3v}$$

Where ω and v are the natural frequency and poisson ratio respectively.

By utilizing Eqs. (22), the TBM equation of motion (17) can be rewritten in dimensionless form

$$e_n{}^4 sbk_G\frac{\partial^8 w}{\partial \zeta^6 \partial \tau^2} - e_n{}^4 sb\frac{\partial^8 w}{\partial \zeta^4 \partial \tau^4}\left(e_n{}^2 + 2e_n{}^2 k_W sb + b + s + sbk_G\right)$$

$$\frac{\partial^4 w}{\partial \zeta^2 \partial \tau^2}$$

$$-e_n{}^2(b + s + e_n{}^2 k_W sb + 2k_W sb)\frac{\partial^6 w}{\partial \zeta^4 \partial \tau^2} + 2e_n{}^2 sb\frac{\partial^6 w}{\partial \zeta^2 \partial \tau^4}$$

$$+ e_n{}^2 k_G s\frac{\partial^6 w}{\partial \zeta^6}$$

$$-(sk_W e_n{}^2 + e_n{}^2 k_G + sk_G + 1)\frac{\partial^4 w}{\partial \zeta^4} - sb\frac{\partial^4 w}{\partial \tau^4}$$

$$+ \left[k_W\left(s - e_n{}^2\right) + k_G\right]\frac{\partial^2 w}{\partial \zeta^2}$$

$$-(sbk_W + 1)\frac{\partial^2 w}{\partial \tau^2} + p\frac{\partial^2 r}{\partial \zeta^2} + pse_n{}^2\frac{\partial^6 r}{\partial \zeta^6} - \frac{\partial^4 r}{\partial \zeta^4}\left(pe_n{}^2 + sp\right)$$

$$\int_0^1 \frac{\partial r}{\partial \zeta}\frac{\partial w}{\partial \zeta} d\zeta$$

$$+ psb\left(e_n{}^4\frac{\partial^6 r}{\partial \zeta^6} - 2e_n{}^2\frac{\partial^4 r}{\partial \zeta^4} + 1\right)\int_0^1 \frac{\partial r}{\partial \zeta}\frac{\partial^3 w}{\partial \zeta \partial \tau^2} dx - k_W w \tag{23}$$

Moreover, the non-dimensional EBM governing equation is obtained from Eq. (19) as

$$\frac{\partial^4 w}{\partial \xi^4} + \frac{\partial^2 w}{\partial \tau^2} - e_n{}^2\frac{\partial^4 w}{\partial \xi^2 \partial \tau^2} + k_G\left(\frac{\partial^4 w}{\partial \xi^4} - e_n{}^2\frac{\partial^2 w}{\partial \xi^2}\right)$$

$$+ k_W\left(w - e_n{}^2\frac{\partial^2 w}{\partial \xi^2}\right) = s\left(\frac{\partial^2 r}{\partial \zeta^2} - e_n{}^2\frac{\partial^4 r}{\partial \xi^4}\right)\int_0^1 \left(\frac{\partial r}{\partial \xi}\frac{\partial w}{\partial \xi}\right) d\xi \tag{24}$$

The Galerkin method is a powerful solution technique to solve the differential equations. The Galerkin method of decomposition is used to obtain the governing ordinary differential equation (ODE) from a partial counterpart. For one-term approximation the deflection of the beam $w(\xi,\tau)$ separates as

$$w(\xi, \tau) = \phi(\xi).e^{i\Omega \tau} \tag{25}$$

Where $\phi(\xi)$ is the fundamental mode shape for boundary conditions of beam and Ω is the dimensionless natural frequency.

The non-dimensional form of boundary conditions from Eqs. (20) and (21) can be written as

$$\phi = \psi = 0 \quad \xi = 0, 1 \tag{26}$$

For clamped ends and

$$\begin{aligned}
&\phi = 0, \\
&\frac{\partial \psi}{\partial \xi} + e_n{}^2 \left(\Omega^2 \phi - \frac{\partial}{\partial \xi}\left(n_x \frac{\partial r}{\partial \xi} \right) \right. \\
&\left. + b\Omega^2 \frac{\partial \psi}{\partial \xi} + k_W \phi - k_G \frac{\partial^2 \phi}{\partial \xi^2} \right) = 0 \quad \xi = 0, 1
\end{aligned} \tag{27}$$

For pinned ends. Here n_x is the dimensionless axial resultant force expressed as $n_x = N_x L^2 / EI$.

It is interesting to note that there isn't any discrepancy in boundary equations between classical and nonlocal beam theories for simply supported boundary condition (Murmu & Pradhan 2009b). This is in view of $\phi = 0$ at the boundaries. Here the dependency of ϕ and ψ is assumed. Therefore, the nonlocal effects are ignored in the Eq. (27). By using the assumption that $\psi = d\phi/d\xi$, the boundary conditions can be simplified as

$$\phi = \frac{d\phi}{d\xi} = 0 \quad \xi = 0, 1. \tag{28}$$

For clamped ends and

$$\phi = \frac{d^2\phi}{d\xi^2} = 0 \quad \xi = 0, 1. \tag{29}$$

In this study three boundary value problems with immovable ends (one for simply supported beam, the second for double clamped and another for clamped-pinned beam) are considered.

Consequently, $\phi(\xi)$ from the boundary conditions will be obtained as follows

1) A beam clamped at both ends or the clamped–clamped boundary condition (C–C):
$$\begin{aligned}
\phi(\xi) = & \cosh(4.73\xi) - 0.9825 \sinh(4.73\xi) \\
& - \cos(4.73\xi) + 0.9825 \sin(4.73\xi)
\end{aligned} \tag{30}$$

2) A beam clamped at one end and simply supported at the other end, i.e. clamped–pinned condition (C–P):
$$\begin{aligned}
\phi(\xi) = & \cosh(3.92\xi) - 1.0008 \sinh(3.92\xi) \\
& - \cos(3.92\xi) + 1.0008 \sin(3.92\xi)
\end{aligned} \tag{31}$$

3) And a simply supported beam at both ends or pinned–pinned condition (P–P):
$$\phi(\xi) = \sin(3.14\xi) \tag{32}$$

Applying Eqs. (30–32) into partial equations of motion SWCNT and multiplying of the these equations by $\phi(\xi)$

and then integrating over the length of SWCNT, the ODE of motion can be obtained.

Therefore, the following linear fourth-order ODE is obtained from TBM as

$$\left(A\Omega^4 - B\Omega^2 + C \right) q = 0 \tag{33}$$

Where A, B and C are the coefficients of general equation of motion (33) that represented in appendix A. The dimensionless linear fundamental frequency represented as

$$\Omega_{TBM} = \frac{1}{2} \left(B - \sqrt{B^2 - 4AC} \right). \tag{34}$$

Similarly, by applying the EBM for the free vibration of a curved SWCNT, the governing equation can be simplified to the following dimensionless equation

$$\left(M_{eq}\Omega^2 + K_{eq} \right) q = 0. \tag{35}$$

Where M_{eq} and K_{eq} are the equivalent of mass and stiffness of the vibrational system that are described in appendix B, and the resonant frequency becomes

$$\Omega_{EBM} = \sqrt{\frac{K_{eq}}{M_{eq}}}. \tag{36}$$

Results and discussion

In this case study, the diameter, aspect ratio, thickness of SWCNT and Young's modulus of the nanotube are assumed to be $d_e = 3.19$ nm, $L/d_e = 6.052$ nm, $t_c = 0.137$ nm, and $E = 2.407$ TPa, respectively (Gupta et al. 2010). The mass density of the SWCNT is 2300 kg/m³ with nonlocal parameter $e_0 a$ of 2 nm. Also, the Winkler modulus and Pasternak modulus are estimated at the values of $K_W = 1$ MPa and $K_G = 5$ nN, in that order (Murmu & Pradhan 2009b). Moreover, the amplitude of curve H is 1 nm (Mayoof & Hawwa 2009).

In order to explore the effects of rotary inertia and transverse shear deformation on the frequency of the curved SWCNT, one makes a comparison between the results obtained from the EBM and TBM as mentioned in Table 1. The values in the brackets are the relative errors between the EBM and TBM. It is found from this table that the resonant frequencies of the TBM are smaller than those predicted by EBM, which overestimates the resonant frequencies for a linear vibration. It is noted that the difference between the values of the resonant frequencies predicted by different beam models in this study is more significant for the stiffer boundary conditions and stocky SWCNTs. In other words, for long and slender SWCNTs with a high aspect ratio, the impacts of transverse shear deformation and rotary

Table 1 Comparison of the dimensionless linear fundamental frequency by TBM and EBM for different boundary conditions and length ($d_e = 3.19$ nm, $H = 1$ nm, $e_0 a = 2$ nm, $K_W = 1$ MPa, $K_G = 5$nN)

boundary condition	L = 20 nm		L = 40 nm		L = 60 nm	
	EBM	TBM	EBM	TBM	EBM	TBM
C-C	17.93	15.19 (15.2%)	21.65	20.94 (3.2%)	22.86	22.58 (1.2%)
C-P	13.24	11.96 (9.7%)	15.71	15.34 (2.3%)	16.65	16.49 (0.9%)
P-P	10.02	9.51(5%)	11.41	11.23 (1.5%)	12.1	12(0.6%)

Figure 3 The difference percent DP against the curvature amplitude *H* for a clamped-clamped SWCNT with different values of the Winkler modulus K_W ($d_e = 3.19$ nm, $e_0 a = 2$ nm, $L/d_e = 6.052$ nm, $K_G = 5$nN).

inertia on the vibration of curved SWCNTs can be ignored, especially for P-P boundary condition.

As mentioned before, another main purpose of this paper is to show the significance of curvature in modeling of the SWCNT vibration. Hence, Figure 2 illustrates the fundamental frequencies of TBM $\Omega_{\mathbf{TBM}}$ against the amplitude of curvature *H* for various boundary conditions. It has been shown from this figure that with increasing the amplitude of waviness *H*, the frequency increases. Furthermore, the fundamental frequencies are completely dependent on the boundary conditions and they are increased while the bending stiffness of the SWCNT rises from P-P to C-C, in particular for low curvature amplitude.
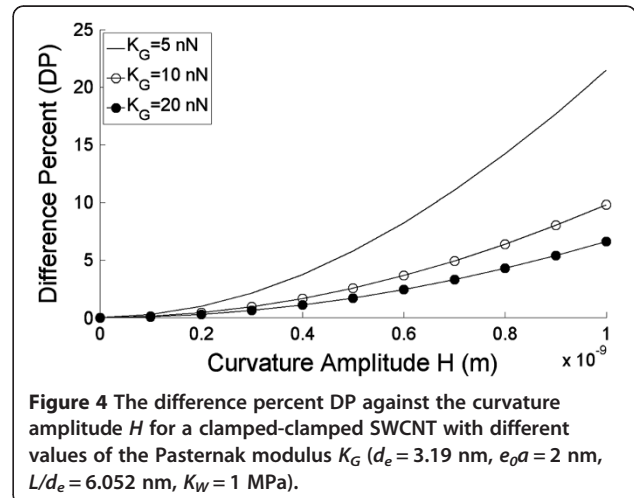
Moreover, to see the effects of curvature clearly, the *difference percent* (DP) is defined as a parameter that shows the percent increment of frequency for a curved SWCNT ($H \neq 0$ nm) compared with a straight nanotube ($H = 0$ nm).
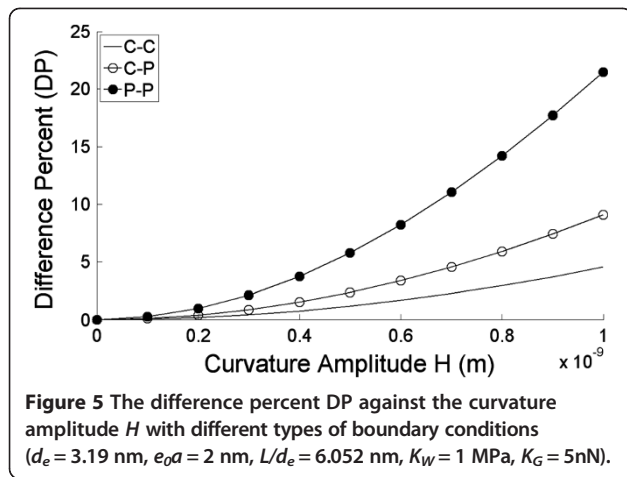
$$DifferencePercent(DP) = \frac{\left(\Omega_{TBM}^{H=Hnm} - \Omega_{TBM}^{H=0nm}\right) \times 100}{\Omega_{TBM}^{H=0nm}}$$

(37)
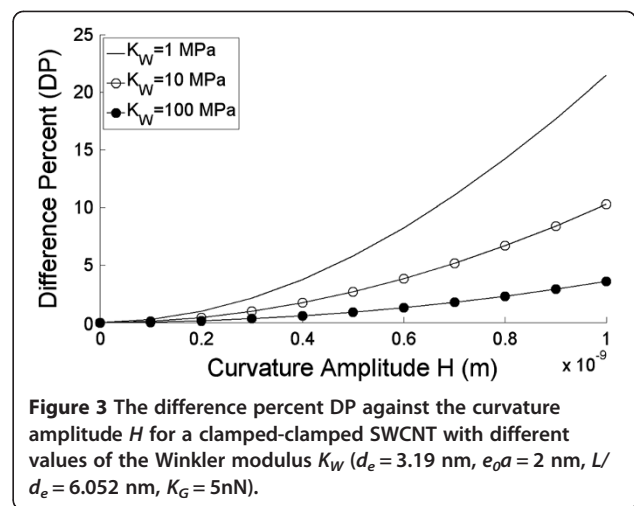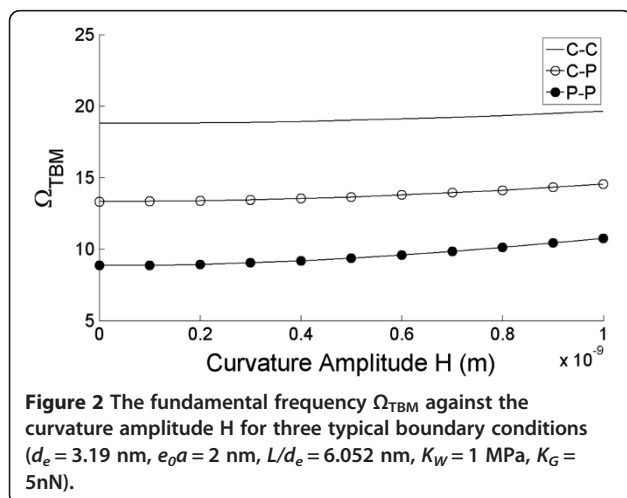
Certainly, DP gives a better illustration for the pure effects of the amplitude of curvature *H*. Figures 3, 4, 5, 6, 7 represent the difference percent DP as a function of the waviness amplitude *H*, while the effects of a certain parameter such as the stiffness of model, the length of SWCNT and the nonlocal parameter have been evaluated in each figure. Obviously, the variation of fundamental frequencies is increased when the waviness is amplified, in all the figures.
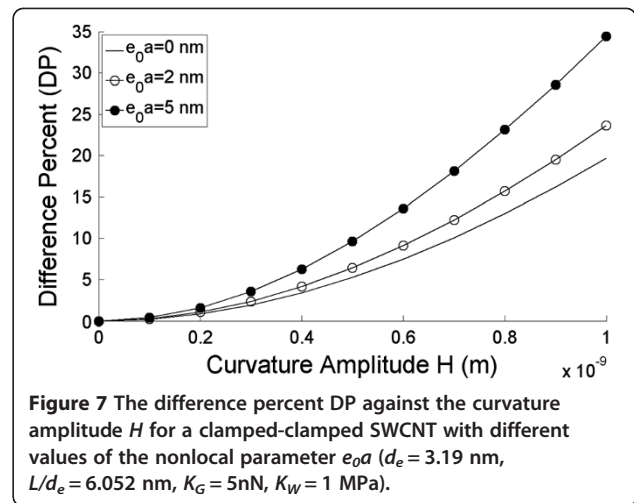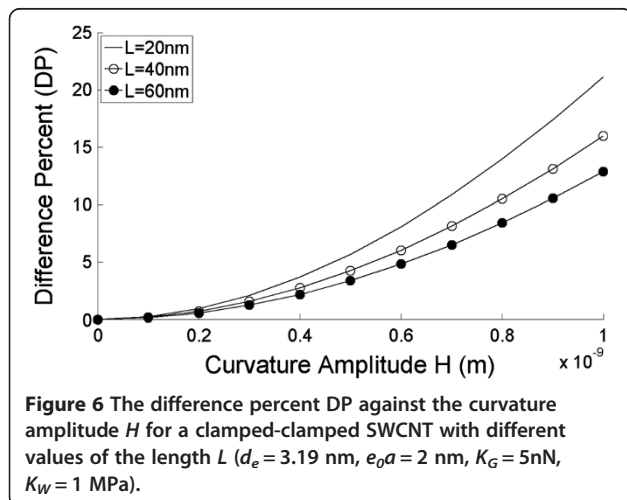
The surrounding elastic medium can be described by Winkler and Pasternak modulus that are determined by the material properties of the elastic medium (Yoon et al. 2003; Lanir & Fung 1972). The DP is very responsive to the stiffness of the model, due to foundation and boundary conditions. As the Winkler modulus K_W and Pasternak modulus K_G of the surrounding elastic medium increase, the shift of the DP is significant (Figures 3 and 4). Therefore, in a soft elastic medium, the effects of the curvature

Figure 2 The fundamental frequency Ω_TBM against the curvature amplitude H for three typical boundary conditions ($d_e = 3.19$ nm, $e_0 a = 2$ nm, $L/d_e = 6.052$ nm, $K_W = 1$ MPa, $K_G = 5$nN).

Figure 4 The difference percent DP against the curvature amplitude *H* for a clamped-clamped SWCNT with different values of the Pasternak modulus K_G ($d_e = 3.19$ nm, $e_0 a = 2$ nm, $L/d_e = 6.052$ nm, $K_W = 1$ MPa).

Figure 5 The difference percent DP against the curvature amplitude *H* with different types of boundary conditions ($d_e = 3.19$ nm, $e_0 a = 2$ nm, $L/d_e = 6.052$ nm, $K_W = 1$ MPa, $K_G = 5$nN).

Figure 7 The difference percent DP against the curvature amplitude *H* for a clamped-clamped SWCNT with different values of the nonlocal parameter $e_0 a$ ($d_e = 3.19$ nm, $L/d_e = 6.052$ nm, $K_G = 5$nN, $K_W = 1$ MPa).

on the vibration of SWCNT increase. In addition, stiffness of boundaries has a similar behavior as the stiffness of the medium. As mentioned previously, to show the effects of boundary condition, this model solved for P-P, C-P and P-P boundary conditions. Figure 5 indicates that the boundary conditions have considerable effects on the DP. The illustration demonstrates that with decreasing the stiffness of the SWCNT from C-C to P-P, the effects of waviness on vibrational frequency increase.

Figure 6 is presented in order to see the role of the SWCNT dimension. It shows the importance of the SWCNT length in the natural frequency and associated difference percent. Results show that an increase in the slenderness ratio causes the DP to considerably decrease. According to this figure, the rise of frequency with curvature amplitude is found to be significantly dependent on the aspect ratio. It means for a long nanotube, the difference of frequency between the straight SWCNT and curved SWCNT is reduced.

Figure 6 The difference percent DP against the curvature amplitude *H* for a clamped-clamped SWCNT with different values of the length *L* ($d_e = 3.19$ nm, $e_0 a = 2$ nm, $K_G = 5$nN, $K_W = 1$ MPa).

Finally, to investigate the effects of nonlocal theory, the DP is plotted as a function of the curvature amplitude *H* and the nonlocal parameter $e_0 a$, in Figure 7. Nonlocal curves have been plotted for three different $e_0 a$ values. The $e_0 a$ values taken are 0 nm, 2 nm and 5 nm. The nonlocal elasticity theory makes nano-devices more flexible and reduces the stiffness of the SWCNTs. As the figure shows, with an increase in model stiffness, by decreasing the nonlocal coefficient, the DP decreases consequently. Therefore, the larger DP occurred at higher nonlocal values and the nonlocal theory provides a higher sensitivity of curved amplitude for the waviness SWCNT.

Conclusions

The nonlocal Timoshenko beam model (TBM) and Euler-Bernoulli beam model (EBM) have been introduced to analyze the effect of waviness on the curved single-walled carbon nanotube (SWCNT). The surrounding elastic medium is simulated using Winkler and Pasternak models. Comparing the results predicted by these two beam models, it is found that the EBM may provide as accurate results as the TBM for SWCNTs with larger length-to-diameter ratio. However, the Timoshenko beam model is highly recommended for stiffer boundary conditions and stocky SWCNTs due to the effects of shear deformation and rotary inertia. In addition, the results show that the waviness has a significant effect on the vibrational behavior of the SWCNT. Detailed results indicate the influence of the curvature, the stiffness of medium around the SWCNT, the boundary conditions, the length of SWCNT and the nonlocal parameter on the natural frequency. Our investigation demonstrates that increasing the amplitude of curvature causes the fundamental frequency to increase.

Furthermore, with an increase in the stiffness of the model, due to the boundary conditions and the foundation, the length of SWCNT and the nonlocal constant, a higher frequency value is obtained for a curved SWCNT in comparison to a straight SWCNT.

Appendix A
The coefficients of Eq. (33)
C-P condition

$$A = 2 + 46.05e_n^4 + 475.34e_n^2$$

$$B = \frac{475.34e_n^2}{s} + \frac{475.34e_n^2}{b} + \frac{23.02e_n^2}{sb} + 5.99e_n^2\pi^5ph^2$$

$$+ 23.02k_G + 5473.78k_Ge_n^4 + 475.34k_We_n^4 + 2\pi^4k_We_n^2$$

$$+ 2.99e_n^4\pi^7ph^2 + 2k_W + 996.73k_We_n^2 + 2.99e^2\pi^3p$$

$$+ \frac{23.02}{s} + \frac{23.02}{b} + \frac{2}{sb}$$

$$C = \frac{1}{b}\left(23.02k_W + 475.34k_G + 475.34e_n^2k_W + 916.65ph^2 \right.$$

$$\left. + 9047.04e_n^2ph^2 + 5473.78k_Ge_n^2 \right)$$

$$+ \frac{1}{sb}\left(23.02k_G + 475.34 + 2k_W + 475.34e_n^2k_G \right.$$

$$\left. + 92.87ph^2 + 916.65e_n^2ph^2 + 23.02k_We_n^2 \right)$$

C-C condition

$$A = 2 + 49.2e_n^4 + 1001.15e_n^2$$

$$B = \frac{1001.15e_n^2}{s} + \frac{1001.15e_n^2}{b} + \frac{24.6e_n^2}{sb} + 1865.17e_n^2ph^2$$

$$+ 24.6k_G + 12315.84k_Ge_n^4 + 1001.15k_We_n^4$$

$$+ 2051.51k_We_n^2 + 9194.93e_n^4ph^2 + 2k_W + 996.73k_We_n^2$$

$$+ 94.58h^2p + \frac{24.6}{s} + \frac{24.6}{b} + \frac{2}{sb}$$

$$C = \frac{1}{b}\left(24.6k_W + 1001.15k_G + 1001.15e_n^2k_W \right.$$

$$\left. + 932.58ph^2 + 9194.93e_n^2ph^2 + 12315.84k_Ge_n^2 \right)$$

$$+ \frac{1}{sb}\left(24.6k_G + 1001.15 + 2k_W + 1001.15e_n^2k_G \right.$$

$$\left. + 94.58ph^2 + 932.58e_n^2ph^2 + 24.6k_We_n^2 \right)$$

P-P condition

$$A = 2 + 39.47e_n^4 + 194.81e_n^2$$

$$B = \frac{194.81e_n^2}{s} + \frac{194.81e_n^2}{b} + \frac{19.73e_n^2}{sb} + 1922.73e_n^2ph^2$$

$$+ 19.73k_G + 1922.73k_Ge_n^4 + 194.81k_We_n^4 + 429.1k_We_n^2$$

$$+ 9488.33e_n^4ph^2 + 2k_W + 996.73k_We_n^2 + 97.4h^2p$$

$$+ \frac{19.73}{s} + \frac{24.6}{b} + \frac{2}{sb}$$

$$C = \frac{1}{b}\left(19.73k_W + 194.81k_G + 194.81e_n^2k_W + 961.36ph^2 \right.$$

$$\left. + 9488.33e_n^2ph^2 + 1922.73k_Ge_n^2 \right)$$

$$+ \frac{1}{sb}\left(19.73k_G + 194.81 + 2k_W + 194.81e_n^2k_G \right.$$

$$\left. + 97.4ph^2 + 961.36e_n^2ph^2 + 19.73k_We_n^2 \right)$$

Appendix B
The coefficients of Eq. (36)
C-C condition

$$K_{eq} = 1 + 12.3e_n^2$$
$$M_{eq} = 12.3k_We_n^2 + 500.56k_Ge_n^2 + 12.3k_G$$
$$+ 467.53ph^2e_n^2 + k_W + 47.37ph^2 + 500.56$$

C-P

$$K_{eq} = 11.51e_n^2 + 1$$
$$M_{eq} = 237.7e_n^2k_G + 11.5e_n^2k_W + 11.5k_G + k_W$$
$$+ 458.4ph^2e_n^2 + 46.4ph^2 + 237.7$$

P-P

$$K_{eq} = 9.8e_n^2 + 1$$
$$M_{eq} = 97.4e_n^2k_G + 9.8e_n^2k_W + 9.8k_G + k_W$$
$$+ 480.6ph^2e_n^2 + 48.7ph^2 + 97.4$$

Author details
[1]Department of Mechanical Engineering, Semnan Branch, Islamic Azad University, Semnam, Iran. [2]Department of Mechanical Engineering, Ferdowsi

University of Mashhad, Mashhad, Iran. [3]Young Researchers Club, Semnan Branch, Islamic Azad University, Semnam, Iran.

References

Iijima S (1991) Helical microtubes of graphitic carbon. Nature 354:56–58

Dresselhaus MS et al (2004) *Electronic, thermal and mechanical properties of carbon nanotubes.* Philosophical Transactions of the Royal Society of London. Ser A Math Phys Eng Sci 362(1823):2065–2098

Treacy MMJ, Ebbesen TW, Gibson JM (1996) Exceptionally high Young's modulus observed for individual carbon nanotubes. Nature 381(6584):678–680

Walgraef D (2007) On the mechanics of deformation instabilities in carbon nanotubes. Eur Phys J Spec Top 146(1):443–457

Chen L et al (2004) Single-Walled Carbon Nanotube AFM Probes: Optimal Imaging Resolution of Nanoclusters and Biomolecules in Ambient and Fluid Environments. Nano Lett 4(9):1725–1731

Hafner JH, Cheung CL, Lieber CM (1999) Growth of nanotubes for probe microscopy tips. Nature 398(6730):761–762

Nishide D et al (2003) High-yield production of single-wall carbon nanotubes in nitrogen gas. Chem Phys Lett 372(1–2):45–50

Tsukagoshi K et al (2002) Carbon nanotube devices for nanoelectronics. Physica B 323(1–4):107

Lau K-T et al (2004) On the effective elastic moduli of carbon nanotubes for nanocomposite structures. Compos Part B Eng 35(2):95–101

Liew KM, He XQ, Wong CH (2004) On the study of elastic and plastic properties of multi-walled carbon nanotubes under axial tension using molecular dynamics simulation. Acta Mater 52(9):2521–2527

Yoon J, Ru CQ, Mioduchowski A (2005) Vibration and instability of carbon nanotubes conveying fluid. Compos Sci Technol 65(9 SPEC. ISS):1326–1336

Zhang YY, Wang CM, Tan VBC (2006) Effect of omitting terms involving tube radii difference in shell models on buckling solutions of DWNTs. Comput Mater Sci 37(4):578–581

Wang L et al (2008) The thermal effect on vibration and instability of carbon nanotubes conveying fluid. Phys E 40(10):3179–3182

Kuang YD et al (2009) Analysis of nonlinear vibrations of double-walled carbon nanotubes conveying fluid. Comput Mater Sci 45(4):875–880

Yakobson BI et al (1997) High strain rate fracture and C-chain unraveling in carbon nanotubes. Comput Mater Sci 8(4):341–348

Nguyen HLT, Elishakoff I, Nguyen VT (2009) Buckling under the external pressure of cylindrical shells with variable thickness. Int J Solid Struct 46(24):4163–4168

Yan Y, Wang WQ, Zhang LX (2009) Dynamical behaviors of fluid-conveyed multi-walled carbon nanotubes. Appl Math Model 33(3):1430–1440

Liew KM, Wang Q (2007) Analysis of wave propagation in carbon nanotubes via elastic shell theories. Int J Eng Sci 45(2–8):227–241

Fu YM, Hong JW, Wang XQ (2006) Analysis of nonlinear vibration for embedded carbon nanotubes. J Sound Vib 296(4–5):746–756

Chaterjee S, Pohit G (2009) A large deflection model for the pull-in analysis of electrostatically actuated microcantilever beams. J Sound Vib 322(4–5): 969–986

Chowdhury R, Adhikari S, Mitchell J (2009) Vibrating carbon nanotube based bio-sensors. Phys E 42(2):104–109

Hsu J-C, Chang R-P, Chang W-J (2008) Resonance frequency of chiral single-walled carbon nanotubes using Timoshenko beam theory. Phys Lett A 372 (16):2757–2759

Wang CM, Tan VBC, Zhang YY (2006) Timoshenko beam model for vibration analysis of multi-walled carbon nanotubes. J Sound Vib 294(4–5):1060–1072

Lee H-L, Chang W-J (2009) A closed-form solution for critical buckling temperature of a single-walled carbon nanotube. Phys E 41(8):1492–1494

Mahdavi MH, Jiang LY, Sun X (2011) Nonlinear vibration of a double-walled carbon nanotube embedded in a polymer matrix. Phys E 43(10):1813–1819

Rao S (2007) Vibration of continuous systems. Wiley, Hoboken, New Jersey

Eringen AC (1983) On differential equations of nonlocal elasticity and solutions of screw dislocation and surface waves. J Appl Phys 54(9):4703–4710

Murmu T, Pradhan SC (2009a) Thermo-mechanical vibration of a single-walled carbon nanotube embedded in an elastic medium based on nonlocal elasticity theory. Comput Mater Sci 46(4):854–859

Şimşek M (2011) Vibration analysis of a single-walled carbon nanotube under action of a moving harmonic load based on nonlocal elasticity theory. Phys E 50:2112–2123

Mehdipour I, Barari A, Domairry G (2011) Application of a cantilevered SWCNT with mass at the tip as a nanomechanical sensor. Comput Mater Sci 50: 1830–1833

Wang L, Ni Q (2008) On vibration and instability of carbon nanotubes conveying fluid. Comput Mater Sci 43(2):399–402

Yang J, Ke LL, Kitipornchai S (2010) Nonlinear free vibration of single-walled carbon nanotubes using nonlocal Timoshenko beam theory. Phys E 42 (5):1727–1735

Murmu T, Pradhan SC (2009b) Buckling analysis of a single-walled carbon nanotube embedded in an elastic medium based on nonlocal elasticity and Timoshenko beam theory and using DQM. Phys E 41(7):1232–1239

Joshi AY, Sharma SC, Harsha SP (2010) Dynamic Analysis of a Clamped Wavy Single Walled Carbon Nanotube Based Nanomechanical Sensors. J Nanotechnol Eng Med 1(3):031007–7

Hawwa MA, Mayoof FN (2009) Nonlinear oscillations of a carbon nanotube resonator. International Symposium on Mechatronics and its Applications, Sharjah

Eringen AC (2002) Nonlocal continuum field theories. Springer Verlag

Gupta SS, Bosco FG, Batra RC (2010) Wall thickness and elastic moduli of single-walled carbon nanotubes from frequencies of axial, torsional and inextensional modes of vibration. Comput Mater Sci 47(4):1049–1059

Mayoof FN, Hawwa MA (2009) Chaotic behavior of a curved carbon nanotube under harmonic excitation. Chaos Solitons Fractals 42(3):1860–1867

Yoon J, Ru CQ, Mioduchowski A (2003) Vibration of an embedded multiwall carbon nanotube. Compos Sci Technol 63(11):1533–1542

Lanir Y, Fung YCB (1972) Errata on "Fiber Composite Columns Under Compression" J. COMPOSITE MATERIALS, Vol. 6 (July 1972), pp. 387–401. J Compos Mater 6(4):533–535